



LAWRENCE
LIVERMORE
NATIONAL
LABORATORY

Water Vapor Transmission Rate Measurement for Moisture Barriers Using Infrared Imaging

M. Bora, R. Gee, Z. Pan, R. Dauskardt

June 15, 2024

Materials Chemistry and Physics

Disclaimer

This document was prepared as an account of work sponsored by an agency of the United States government. Neither the United States government nor Lawrence Livermore National Security, LLC, nor any of their employees makes any warranty, expressed or implied, or assumes any legal liability or responsibility for the accuracy, completeness, or usefulness of any information, apparatus, product, or process disclosed, or represents that its use would not infringe privately owned rights. Reference herein to any specific commercial product, process, or service by trade name, trademark, manufacturer, or otherwise does not necessarily constitute or imply its endorsement, recommendation, or favoring by the United States government or Lawrence Livermore National Security, LLC. The views and opinions of authors expressed herein do not necessarily state or reflect those of the United States government or Lawrence Livermore National Security, LLC, and shall not be used for advertising or product endorsement purposes.

Water Vapor Transmission Rate Measurement for Moisture Barriers Using Infrared Imaging

Ziyi Pan, Mihail Bora, Richard Gee, Reinhold H. Dauskardt**

Ziyi Pan

Department of Chemistry

Stanford University, Stanford, CA 94305-2205, United States

Mihail Bora

Lawrence Livermore National Laboratory, CA 94550, United States

E-mail: bora1@llnl.gov

Richard Gee

Lawrence Livermore National Laboratory, CA 94550, United States

Reinhold H. Dauskardt

Department of Materials Science and Engineering

Stanford University, Stanford, CA 94305-2205, United States

E-mail: rhd@stanford.edu

LLNL-JRNL-865629

Abstract

Here we demonstrate a spatially resolved imaging methodology for water vapor transmission rate (WVTR) testing that relies on quantified infrared characterization at water absorption bands. This technique is validated using a moisture barrier on a polymer substrate via calibration of the infrared image intensity with moisture content in the polymer substrate from images taken at different times. The method is compared to existing state of the art techniques such as membrane permeation measurement with coulometric phosphorous pentoxide sensor and optical calcium film testing. This fast, non-destructive and in-situ method enables defect visualization and shows the WVTR with a sensitivity limit of $5 \cdot 10^{-5}$ g/m²/day.

Introduction

Protection from water using moisture barriers is critical to a wide variety of applications, from food and pharmaceutical packaging^{1,2,3} to electronic displays and photovoltaic technologies such as organic light-emitting diodes (OLED)^{4,5} and perovskite solar cells^{6,7}, with varying requirements for the moisture barrier performance. The food packaging industry necessitates materials that have a water vapor transmission rate (WVTR) of 0.1-1 g/m²/day; for thin film photovoltaic devices, the expected WVTR for barrier film needs to be less than 1·10⁻⁴ g/m²/day; OLEDs require barriers with WVTR less than 1·10⁻⁶ g/m²/day^{8,9}.

The development of high-performance moisture barriers requires fast, accurate and reliable testing methodologies for materials and processing parameters optimization. The most used metric representing moisture barrier efficacy is WVTR expressed as the amount of water that passes through the barrier per unit area and unit time and generally measured under constant temperature and humidity conditions. Several methods are currently used to measure WVTR, such as optical and electrical calcium test¹⁰⁻¹³, tritiated water (HTO) permeation test^{14,15}, membrane permeation test with coulometric sensor^{16,17}, quadrupole mass spectrometry (QMS)^{18,19}, and cavity ring-down spectroscopy (CRDS)^{20,21}. Of these, only the optical calcium test provides imaging capabilities to allow moisture barrier defect visualization and screening. In this work, we develop a novel infrared imaging testing methodology for moisture barrier films and provide comparison on imaging capabilities with the optical calcium test and overall WVTR

detection accuracy with both a permeation method using coulometric sensor and the optical calcium test.

The optical calcium test relies on the reaction of water with metallic calcium to determine moisture transmission rates. A layer of calcium is deposited in the proximity of the moisture barrier and sealed from the external environment. When the sample is exposed to water, the conductive and opaque calcium will turn into insulating and transparent calcium hydroxide after reacting with moisture. The WVTR can be assessed either by measuring the change in the area of calcium film or by monitoring the change in the conductance of the calcium layer during the degradation process. Although this test method is widely used, it is time-consuming, and its reproducibility is affected by the quality of the calcium evaporated. Additionally, calcium is extremely sensitive to the atmospheric environment; thus, vacuum condition and glovebox equipment are required for the sample fabrication process, adding inconvenience and cost to the experimental test. Moreover, the kinetics of calcium oxidation is highly dependent on the test setup, and recently calcium test accuracy has been criticized.^{22,23}

Permeation testing is a widely available method for measuring WVTR using commercial instrumentation (Aquatran, Ametek). In this method, the test specimen is held between two test chambers, with one side of the sample exposed to water vapor and the other to dry side purged by inert gas, such that any water detected is introduced through the barrier film carried by inert gas. The WVTR measured with this method has a detection limit of $5 \cdot 10^{-5} \text{ g/m}^2/\text{day}$,^{16,17} adequate for measurement of samples with low WVTR. However, the measured samples need to be cut to fit the test chamber and only one or two samples can be measured at one time, resulting in relatively low throughput.

As each method has significant limitations that include generally low throughput, destructive evaluation, and time-consuming. The calcium test has higher capital equipment costs, tends to have more significant variability and requires specialized testing configurations including the calcium layer. The permeation test while less expensive to implement, does not include imaging capabilities. A higher throughput method with imaging capabilities to assess moisture barriers conveniently and cost-effectively with high throughput and no size limitation is needed.

Here we report a fast, non-destructive and in-situ method by quantifying the infrared radiation attenuation upon moisture absorption into the barrier polymer substrate to calculate the WVTR with a sensitivity limit of $5 \cdot 10^{-5}$ g/m²/day, on par with existing instrumentation. We have demonstrated applicability of the infrared imaging technique by measuring barrier films on polymer substrates providing comparisons to results from permeation and calcium tests.

Methods and materials

Materials

Two commercially available moisture barrier films obtained from manufacturer (Vitriflex, Inc) were selected for WVTR measurement, one comprising 1 μ m SiO₂ evaporated on 125 μ m polyethylene terephthalate (PET) (VitriSol125MDTM, FG 60-R3-S3-31) and the other comprising 1 μ m SiO₂ evaporated on 50 μ m PET (VitriSol50UVTM, FG 261-R1-1). Barrier films of 2 \times 2 cm size were cut from A4 size barrier sheets for sample fabrication process in the following sections.

Infrared imaging testing

The custom-built infrared imaging system is composed of an illumination source, and a camera equipped with a band pass filter centered on a water absorption band between 3500-3700 cm^{-1} , with samples measured either in transflection (forward transmission, reflection off the metallization, and backwards transmission) or transmission modes^{24,25}. The illumination source consists of a wide area black body heated at a constant temperature (125 °C) to increase its thermal emissivity and brightness. A sample of interest is placed such that light emitted by the source is reflected off the samples and imaged by the infrared camera, as shown in **Figure 1a**. The presence of water within the sample can be determined based on the attenuation of the infrared radiation imaged by the detector.

During calibration of the black body at 125°C, it is placed at 30 to 60 cm away from the sample to minimize heating impact on the sample. Typical images are acquired within 5 minutes (including sample positioning, focusing, and imaging). During this time, no change in image intensity was observed.

To generate a calibration curve relating image intensity with moisture content in the polymer substrate, samples (2×2 cm) were fabricated with 1 μm copper thermally evaporated (Angstrom) on the silicon oxide side such that the polymer substrate is easily accessible for moisture diffusion, then followed by epoxy mounting a glass slide on the copper to provide mechanical rigidity. The samples were stored in a glovebox to equilibrate under dry nitrogen or at constant temperature of 30 °C and different relative humidity of 15, 30, 50, 70, and 90% and then imaged with infrared camera.

To measure the WVTR of the moisture barriers, samples (2×2 cm) used in the experiment consisted of a PET substrate with a layer of silicon oxide deposited on top and protected by a removable peel off film. Tested samples were fabricated by thermally evaporating 1 μm copper

onto the PET side followed by epoxy mounting on a glass slide to provide mechanical rigidity, as shown on **Figure 1b**. Barrier samples were aged under 38 °C and 90% relative humidity (R.H.) environmental condition and taken out of the chamber at set intervals and imaged with the infrared camera to monitor and quantify water content in the polymer substrate over time.

Imaging processing

The images acquired from the camera were numerically processed using MATLAB (The MathWorks, Inc) to generate a calibration curve relating image intensity with water content in the polymer substrate. The relevant section of the image representing the sample was identified by pixels with intensity above a background threshold. Then, the corresponding sample intensity was calculated by taking the average of all pixels within the domain and then fitted with a linear dependence against the water concentration measured by Karl Fischer titration to determine the slope of image intensity vs. water concentration as following equation:

$$slope = \frac{\Delta Intensity}{\Delta conc_{water}} \quad (1)$$

The images taken for WVTR calculation were first normalized between the image minimum corresponding to background (not belonging to the image) and the maximum of the image corresponding to an area where water does not diffuse during environmental exposure. For each of the normalized images, the average intensity was calculated by manually excluding the perimeter area that corresponds to diffusion from the perimeter and is not representative of diffusion across the barrier. The decrease in image intensity between different time points was converted to increase in water content through the slope of the calibration curve, and further converted to water vapor transmission rate by normalization with respect to area and time using the following equation:

$$WVTR (g m^{-2} day^{-1}) = \frac{\Delta mass_{water}}{t \cdot A} \quad (2)$$

where $\Delta mass_{water}$ is the mass of water increase in the polymer substrate over the testing time, t is the testing time, and A is the area of the barrier sample.

Karl Fischer titration

The absolute moisture content in the PET substrate was determined with Karl Fischer titration (Metrohm) by equilibrating samples at constant temperature (30 °C) and different relative humidity of 15, 30, 50, 70, and 90%. The samples were then transferred into glass vials and sealed with a septum cap, then heated to 150 °C to release the moisture dissolved in the polymer and further transferred to an electrochemical reaction chamber where the total amount of water was measured. The concentration of water was then expressed as a percentage by taking the ratio between measured water mass and the mass of the dried polymer film (dry basis percentage).

Fourier transform infrared (FTIR) spectroscopy

To demonstrate the spectroscopic basis of the infrared imaging, FTIR spectroscopy measurement was conducted on samples fabricated with 1 μm copper deposited on the silicon oxide side such that the substrate is easily accessible for moisture diffusion. The samples were equilibrated under the same conditions as the Karl Fischer titration conditions at 30 °C and relative humidity of 15, 30, 50, 70 and 90%. For each condition the infrared reflectivity of the sample was measured in transflection mode (incident light passing twice through the polymer and reflecting off the copper metallization) on an instrument covering the near infrared spectrum (Bruker, Billerica MA). The angle of incidence for the measurement was 11 deg, comparable to

the angle of view for the infrared imaging. The spectra exhibited interference fringes from the air/polymer and copper/silicon oxide interfaces, that were removed with a numerical data processing algorithm for clarity. The procedure involves performing a Fourier transform of the transfection spectrum, identifying the coefficients that contribute the interference pattern, setting them to zero, and then performing an inverse Fourier transform to obtain the spectrum without interference fringes.

Permeation testing

Permeation testing was performed in an Aquatran instrument (Ametek) where the test cell was divided into two chambers by a sample film of size 50 cm². In one chamber, a constant condition with temperature of 38 °C and relative humidity of 90% was maintained. In the second chamber, a dry environment with 0% relative humidity was sustained via purging dry nitrogen carrier gas, which guides the permeated water molecules to the coulometric phosphorous pentoxide sensor. Measurements were taken every 4 hours for a total time interval of 60 hours with the silicon oxide side of the barrier film facing toward the dry nitrogen purged low humidity chamber.

Optical Calcium Film Testing

The samples for calcium testing were fabricated by deposition of a 3 by 3 array of 3mm-by-3mm squares of 50 nm calcium on the 2×2 cm silicon oxide barrier side of the samples followed by thermal evaporation of a 1µm copper film enclosed in a dry nitrogen environment glovebox. Then, the samples were sealed using epoxy and attached to a glass slide for mechanical rigidity. Sample was aged in a 38°C and 90% R.H environmental chamber and imaged with a consumer grade camera at regular intervals. Then, images were digitally

processed via MATLAB by selecting the blue color channel of the RGB images with a threshold binarization to convert the image into a map of reacted calcium and calculating the WVTR using the following equation:

$$WVTR (g m^{-2} day^{-1}) = n \cdot \delta_{Ca} \cdot \frac{MW_{water}}{MW_{Ca}} \cdot h \cdot \frac{dA}{dt} \cdot \frac{1}{A} \quad (3)$$

where n is molar ratio of water to calcium in the calcium oxidation reaction, δ_{Ca} is the calcium density (1.55 g cm^{-3}), MW_{water} and MW_{Ca} are the molar mass of water and calcium respectively, h is calcium film thickness, dA/dt is the rate of change of the area of the calcium square, and A is the area of the evaporated calcium square (9 mm^2).

Results

To develop a quantitative WVTR testing method, water absorption properties of the PET polymer substrate were characterized with Karl Fisher titration, FTIR and infrared imaging after equilibration in identical conditions at $30 \text{ }^\circ\text{C}$ and relative humidity of 15, 30, 50, 70, 90%. A calibration curve was developed to relate the image intensity with the water concentration in the PET substrate, such that quantitative measurements of water content are derived from the infrared image intensity data.

Figure 2a presents the dependence of the absolute water content in the PET substrate measured with Karl Fischer titration as a function of relative humidity equilibration conditions. The water content vs. relative humidity data points were fit with a linear dependence to estimate the water concentration for other relative humidity values. The increase in spectroscopic absorbance of the infrared region for the PET barriers substrate upon moisture uptake were measured with a FTIR instrument configured in transfection mode between $3700\text{-}3500 \text{ cm}^{-1}$ as

shown in **Figure 2b**. The integration of water absorption band is shown on **Figure 2d** as a function of absolute water concentration in the substrate measured with Karl-Fisher titration indicating a good linear fit.

Figure 2c shows the images taken under these conditions indicating a decrease in image intensity due to water uptake in the PET substrate, with a similar mechanism responsible for the decrease in FTIR transfection spectra. Lower water content results in samples with a brighter appearance when imaged with the infrared camera due to less light being absorbed by the water dissolved in the polymer substrate. The samples have a uniform appearance indicating negligible variations in polymer thickness and the concentration of water across the entire area. The average intensity value of the substrate for each relative humidity condition was plotted against the corresponding water content measured with the Karl Fisher titration method (**Figure 2d**) showing a linear dependence with a good fit. With this calibration, the water content in the substrate can be correlated to a specific image intensity average which can be further used to calculate the water vapor transmission rate of the moisture barrier films. The key parameter derived from the calibration is the slope of the fit as shown in equation (1), which relates the intensity changes in the barrier samples to the absolute water content that diffused into the polymer substrate. In its simplest form, the intensity-water content calibration can be performed with only two images (e. g. equilibrating under 0% and 90% relative humidity respectively) allowing a straightforward calculation of the slope.

Moisture barrier films (VitriSol125MDTM, FG 60-R3-S3-31) with higher WVTR have been evaluated with the IR imaging system to demonstrate the visualization of defects after water diffusion through the inorganic film composing the sample. The surface quality was also assessed under bright illumination which exhibited light scattering, possibly indicating

microscopic pinholes and scratches. Although it is difficult to evaluate from the infrared image alone how these defects contribute to an increase in the WVTR, the defects in the barrier are readily identified from the infrared images after accelerated ageing exposure. **Figure 3a** shows the infrared images of the barrier film exposed in environmental chamber at 38°C, 90% relative humidity for different times, with the most obvious degradation behavior correlated with the appearance of defects, such as pinholes and scratches on the silicon oxide moisture barrier layer. Since the sides were not protected with edge seal, diffusion from the perimeter can be identified as a darker band at the edge that decreased in intensity over longer exposure time in the environmental chamber. To measure the water vapor transmission rates through the barrier alone, the sample can be sealed around the edges, or as a simpler alternative that was followed in this work, digitally excluded the edges from analysis the portion of the sample where the edge diffusion of water occurred. Microscopic defects in the barrier can be visualized from their water diffusion footprint, appearing as dark spots with an increasing size as more water diffused into the sample. Scratches were identified as dark longitudinal segments with increasing apparent darkness over longer moisture exposure time. These results highlighted a straightforward surveillance of defect shape, size, and distribution that in some cases can be sufficient for a qualitative evaluation of moisture barrier performance.

A quantitative image analysis indicated a decrease in intensity over time (**Figure 3b**) due to water transport through several distinct pathways: diffusion from the edges, through barrier defects that result in a microscopic footprint, and through nanoscale size defects or porosity that result in a uniform diffusion over the entire barrier area. Samples kept in the environmental chamber for longer time absorbed more moisture, resulting in decreased image intensity due to the infrared absorption by water.

A different set of barrier film (VitriSol50UVTM, FG 261-R1-1) was tested to evaluate the lower limit of detection for measuring WVTR with the infrared imaging system, as the previous sample (**Figure 3**) has an estimated WVTR of $1 \cdot 10^{-2}$ g/m²/day, which is more appropriate for highlighting defects that result in water diffusion into the substrate. Sequential infrared images of the samples were acquired every 24 hours after exposure in 38 °C and 90% R.H. environmental chamber as shown in **Figure 4a**, indicating a decrease in intensity over longer aging time. Qualitatively, this barrier film sample shows fewer defects in the infrared images indicating better performance. As for the previous sample, diffusion from the unsealed edges can be seen clearly as a dark band around the perimeter. To calculate WVTR value of the barrier sample, a strip around the perimeter corresponding to edge diffusion, approximately 4 mm wide, was digitally excluded from the analysis and only the center of the sample was selected to calculate the average image intensity for each measurement as shown in **Figure 4b**. Then, the amount of water diffused into the sample was calculated from the slope of the calibration curve relating the change in intensity with respect to the change in water concentration in the sample. Finally, the WVTR was calculated as the flux of water diffusing across the inorganic barrier into the polymer substrate using equation (2) with the result value of $9.6 \cdot 10^{-4}$ g/m²/day.

The moisture diffusion process into the barrier was modelled using a one-dimensional Fick's second law, that consists of a 1 μm thick silicon oxide barrier layer on top of a 50 μm thick PET substrate. The boundary conditions are set at water saturation concentration at the silicon oxide barrier side exposed to humid air, and no water flux on the PET substrate side that is sealed with a uniform copper layer. At the interface between the barrier and substrate, the concentration of water relative to saturation concentration is assumed to be continuous as shown on **Figure 5a**. The model was used to fit the experimental results by applying least square

analysis via minimizing the difference between water concentrations predicted by the model and the ones derived from infrared imaging. The diffusion coefficient of the PET polymer substrate was set to be $8.5 \cdot 10^{-9} \text{ cm}^2/\text{s}$ as shown in literature.^{26,27} This procedure provides the diffusion coefficient of the inorganic barrier as $8 \cdot 10^{-15} \text{ cm}^2/\text{s}$ that is further used in the model to generate the fit shown in **Figure 5b**. The transportation of water through the low diffusion coefficient moisture barrier layer to the PET substrate layer results in a lag time for about 2 days from the modelling, a feature that was not observed obviously from the experimental results, possibly due to a small fraction of water diffusing into the barrier during sample transfer at the beginning or suggesting that water diffusion through the barrier layer possibly occurred through a fraction of high permeation areas distributed across the sample. The data was fitted with numerical results after the two-day lag time for better agreement with the experimental results and also providing a single value diffusion coefficient reflecting silicon oxide barrier layer water transport property. **Figure 5c** shows the water concentration profile in the sample where the water diffusion front passes through the barrier layer until it reaches a linear profile take approximately 4 days. The moisture diffusion is limited by transportation through the silicon oxide barrier layer and the concentration across the PET substrate is constant due to the fast diffusion of water in this material.

The moisture barrier was also evaluated with permeation measurement to determine the steady state WVTR at 38 °C when one side of the barrier sample was exposed to 90% relative humidity and the other side to dry nitrogen. Under these conditions, moisture permeation through the barrier equilibrated within 4-hour exposure reaching steady state for the moisture gradient across the barrier substrate, after which the WVTR is relatively constant (**Figure 6a**). The average WVTR was measured at $1.7 \cdot 10^{-4} \text{ g/m}^2/\text{day}$, with a coefficient of variation of 18%.

The infrared imaging method for measuring WVTR was also compared with optical calcium test, one of the most common WVTR measurement alternatives, to demonstrate the accuracy and highlight the benefits of our approach. The area of calcium films that reacted with water diffusing through barrier film as a function of exposure time to the same aging condition (38 °C and 90 % R.H.) is shown in **Figure 6b**. The WVTR was then calculated via the rate of reacted Ca area change over 10-day measurement and further normalized to unit time and area as shown in Equation (3) resulting in WVTR value of $8.5 \cdot 10^{-4}$ g/m²/day.

Table 1 shows comparison of the WVTR results for a same barrier sheet measured with IR imaging, permeation test, and optical calcium film test. The WVTR values determined using the novel infrared imaging approach agreed with those measured using a commercially available permeation instrumentation and are close to the result measured from optical calcium film testing.

Discussion

We chose the two most established methods, permeation testing and optical calcium testing, to compare with the IR imaging method for measuring WVTR of commercially available moisture barrier samples. The three different measurement techniques are performed with different principles under distinct boundary conditions corresponding to no moisture flux for the sealed polymer substrate (infrared imaging method), zero water concentration (optical calcium test) and steady state (permeation test). It is therefore expected that differences in measured WVTR are present even when measuring the same sample.

For permeation test, the water molecules that pass into the low humidity side is further diluted by carrier gas, and there is a penalty on sensitivity as the sensor needs to test a larger volume compared to the case when the water is accumulated inside the sample. The permeation measurement outputs a global average value for the WVTR, but it does not provide any information on the characteristics of the defects that contribute to water permeation, such as defect size, density, or location. Additionally, the permeation test measures water diffusion under steady state, a condition that is rarely encountered for barrier films during field deployment. The most obvious weakness of permeation testing is its low throughput, with WVTR close to the detection limit of $5 \cdot 10^{-5}$ g/m²/day taking days to complete the testing.

Optical calcium test was also compared to infrared imaging method for measuring the WVTR of moisture barriers. As the analysis is based on reaction between water and calcium and its conversion to calcium hydroxide, the test only detects water molecules that contribute to this reaction. At longer exposure times, as the calcium hydroxide area is growing, it is possible that more water is present between the defect sites and the reacted front in the calcium film that cannot be detected resulting in lower calculated WVTR values. Moreover, the calcium film can be partially reacted and not pass the detection threshold for image binarization indicating the possibility that a fraction of water diffusing into the barrier is not accounted for in an optical calcium test, which can also lead to inaccurate WVTR estimation. The optical calcium test exhibited the most variability with some samples having the calcium film completely reacted, while others showing no obvious sign of moisture damage, likely related to the small tested sample area of 9 mm².

WVTR measurements using infrared imaging ($9.6 \cdot 10^{-4}$ g/m²/day), optical Ca test ($8.5 \cdot 10^{-4}$ g/m²/day) and permeation method ($1.7 \cdot 10^{-4}$ g/m² /day) showed comparable results with each

other. It is worth noting that the variability in WVTR values obtained from different methodologies is common in moisture barrier property studies. Even if using the same technique under identical testing condition to evaluate the same barrier sheet, there could be a factor of 3 difference in the WVTR values due to variations in the defect densities present in different test samples.^{21,28,29} Therefore, due to the infrared imaging measurements involving multiple images indicating the measurement variability as well as sample-to-sample variations, one sample of each barrier was measured for WVTR calculation.

In this work we developed an alternative to the permeation test and optical calcium film test for measuring the WVTR of moisture barriers that combines the benefits of both approaches and is based on high absorbance of water in the infrared region of the spectrum. The hydroxyl groups in water absorb incident light around the 3500 cm^{-1} band, resulting in a decrease in image intensity captured by the camera detector. A calibration curve is established for the polymer substrate to derive the WVTR value. The infrared imaging provides localized information of water content based on the absorption of the diffused water, and in this aspect, it is similar to defect identification revealed by reacted optical calcium films; in contrast, the permeation measurement provides only a global WVTR value, with little insight on spatial distribution of defects. For both infrared imaging and optical calcium test, the water is accumulated within the testing area, while for permeation method the water is diluted and carried to the sensor. The sample preparation is simplest for permeation because it requires no additional fabrication, infrared imaging requires one single step of sealing the back side of the barrier with a metal layer, while calcium film requires patterned deposition, backside and edge side sealing, all steps being done in inert atmosphere as calcium is sensitive to atmospheric oxygen and water. Edge seals were deliberately not included for the infrared imaging to demonstrate that accurate WVTR

data can be determined with minimal sample edges easily excluding from the analysis, which is a significant advantage compared to the calcium film testing.

The limit of detection is estimated around $5 \cdot 10^{-5}$ g/m²/day from the infrared intensity resolution of 1 count per pixel, which was extrapolated from the barrier testing given the instrumentation capabilities and characteristics. For the WVTR of $\sim 5 \cdot 10^{-4}$ g/m²/day measured in this work, it was observed an average change in the image intensity of 10 counts. Therefore, it is estimated that the instrument can detect average change of 1 count to infer a limit of detection that is 10 times lower at $5 \cdot 10^{-5}$ g/m²/day. In practice, measuring low WVTR is dependent on sample, this limit of detection can be improved if the water transport mechanism across the barrier is dominated by pinholes, the high concentration of water near defect can be measured with higher accuracy, hence the detection limit will be lower compared to uniform permeation barrier samples.

Of the three methods, infrared imaging is the most cost-effective, as calcium test requires significant capital investment (glove box, evaporation system) and operational costs, while the permeation measurement suffers from low throughput. In contrast, infrared imaging only requires a light source and a camera, with testing taking only minutes. The infrared imaging is also the most flexible testing method, as it allows samples of any size, and exposure conditions to a wide range of aging parameters. For permeation test, the sample size is set to the chamber area, a circle of 50 cm², while the environmental exposure to temperature and humidity is limited by the instrument capabilities and spans a narrower range compared to commonly used environmental chambers. Measurement precision and reliability was best for permeation testing and infrared imaging method, while optical calcium film testing required a significant amount of user input for image analysis in determining the threshold for considering completely reacted

calcium film. In addition, if the edge is not protected, poor adhesion between calcium and silicon dioxide barrier layer results in fast reaction from the edge, rendering the test unusable. The most significant disadvantage of the infrared imaging approach is that it requires additional testing to determine the slope of the calibration curve relating image intensity with absolute water content for quantitative WVTR measurement. At the minimum, a two-point calibration is sufficient to determine the slope of image intensity versus concentration, with one image equilibrating under 0% R.H. and the other under 90% R.H.

The infrared imaging approach for WVTR measurement offers significant benefits compared to existing methods in terms of performance, effectiveness and convenience. The measurement can be done on large size samples with a relatively easy preparation process, no need for edge diffusion protection and glovebox handling and fabrication environment. It can be used qualitatively to visualize defects or quantitatively to determine the WVTR in conjunction with a calibration process relating image intensity with water concentration.

Conclusion

This work demonstrates the use of an infrared imaging system to measure the performance of ultrahigh moisture barriers to an estimated detection limit of $5 \cdot 10^{-5}$ g/m²/day, on par with commercial instrumentation. Measurements can be performed over a broad range of sample sizes, temperatures, and relative humidity conditions. A comparison of WVTR results from optical calcium test and permeation method, both based on different operational principles, confirms the accuracy of the infrared imaging approach, and highlights the benefits of non-destructive and in-situ evaluation for water transport properties in moisture barriers. The

technique has a wide sensitivity range, is easy to employ, and amenable to measuring large sample sizes, making the IR imaging a candidate to replace existing moisture barrier testing methodologies.

Acknowledgements

This work was funded as part of the Durable Modules Materials Consortium (DuraMAT), an Energy Materials Network Consortium funded by the US Department of Energy, Office of Energy Efficiency and Renewable Energy, Solar Energy Technologies Office agreement number 32509.

References

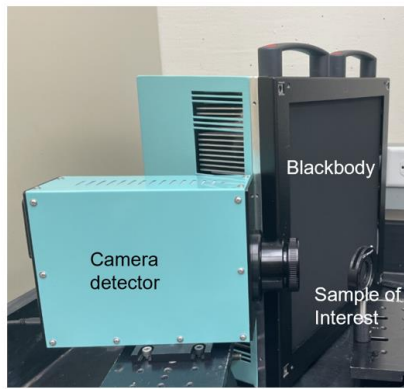
1. Yu, J., Ruengkajorn, K., Crivoi, DG. *et al.* High gas barrier coating using non-toxic nanosheet dispersions for flexible food packaging film. *Nat Commun* **10**, 2398 (2019).
2. Nguyen, H.-L.; Tran, T. H.; Hao, L. T.; Jeon, H.; Koo, J. M.; Shin, G.; Hwang, D. S.; Hwang, S. Y.; Park, J.; Oh, D. X. Biorenewable, Transparent, and Oxygen/Moisture Barrier Nanocellulose/Nanochitin-Based Coating on Polypropylene for Food Packaging Applications. *Carbohydrate Polymers* **2021**, 271, 118421.
3. Yang, Q.; Yuan, F.; Xu, L.; Yan, Q.; Yang, Y.; Wu, D.; Guo, F.; Yang, G. An Update of Moisture Barrier Coating for Drug Delivery. *Pharmaceutics* **2019**, 11 (9), 436.
4. Lim, S. F.; Wang, W.; Chua, S. J. Degradation of Organic Light-Emitting Devices Due to Formation and Growth of Dark Spots. *Mater. Sci. Eng., B* 2001, 85, 154–159.
5. Wu, J.; Fei, F.; Wei, C.; Chen, X.; Nie, S.; Zhang, D.; Su, W.; Cui, Z. Efficient Multi-Barrier Thin Film Encapsulation of OLED Using Alternating Al₂O₃ and Polymer Layers. *RSC Advances* **2018**, 8 (11), 5721–5727.
6. Wang, Z.; Shi, Z.; Li, T.; Chen, Y.; Huang, W. Stability of Perovskite Solar Cells: A Prospective on the Substitution of the A Cation and X Anion *Angewandte. Angew. Chem., Int. Ed.* 2017, 56, 1190–1212.
7. Song, Z.; Shrestha, N.; Wathage, S. C.; Liyanage, G. K.; Almutawah, Z. S.; Ahangharnejhad, R. H.; Phillips, A. B.; Ellingson, R. J.; Heben, M. J. Impact of Moisture on Photoexcited Charge Carrier Dynamics in Methylammonium Lead Halide Perovskites. *J. Phys. Chem. Lett.* 2018, 9, 6312–6320.

8. Zhang, K.; Yu, Q.; Zhu, L.; Liu, S.; Chi, Z.; Chen, X.; Zhang, Y.; Xu, J. The Preparations and Water Vapor Barrier Properties of Polyimide Films Containing Amide Moieties. *Polymers* **2017**, *9* (12), 677.
9. With, P. C.; Helmstedt, U.; Prager, L. Flexible Transparent Barrier Applications of Oxide Thin Films Prepared by Photochemical Conversion at Low Temperature and Ambient Pressure. *Frontiers in Materials* **2020**, *7*.
10. Schubert, S.; Klumbies, H.; Müller-Meskamp, L.; Leo, K. Electrical Calcium Test for Moisture Barrier Evaluation for Organic Devices. *Review of Scientific Instruments* **2011**, *82* (9), 094101.
11. Choi, J. H.; Kim, Y. M.; Park, Y. W.; Huh, J. W.; Ju, B. K.; Kim, I. S.; Hwang, H. N. Evaluation of Gas Permeation Barrier Properties Using Electrical Measurements of Calcium Degradation. *Review of Scientific Instruments* **2007**, *78* (6), 064701.
12. Nisato, G.; Bouten, P. C. P.; Slikkerveer, P. J.; Bennett, W. D.; Graff, G. L.; Rutherford, N.; Wiese, L. Evaluating Higher Performance Diffusion Barriers: The Calcium Test. *Proc. Asia Display/IDW '01 2001*, 1435.
13. Carcia, P. F.; McLean, R. S.; Reilly, M. H.; Groner, M. D.; George, S. M. Ca Test of Al₂O₃ Gas Diffusion Barriers Grown by Atomic Layer Deposition on Polymers. *Applied Physics Letters* **2006**, *89* (3), 031915.
14. A.A. Dameron, S.D. Davidson, B.B. Burton, P.F. Carcia, R.S. McLean, S.M. George, Gas diffusion barriers on polymers using multilayers fabricated by Al₂O₃ and rapid SiO₂ atomic layer deposition, *J. Phys. Chem. C* **112** (2008) 4573–4580.
15. M.D. Groner, S.M. George, R.S. McLean, P.F. Carcia, Gas diffusion barriers on

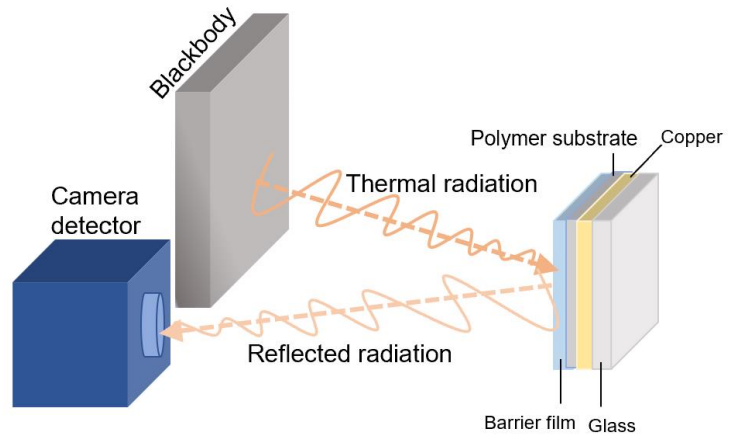
- polymers using Al₂O₃ atomic layer deposition, *Appl. Phys. Lett.* 88 (2006) 051907-051903.
16. T. Ahmadzada, D.R. McKenzie, N.L. James, Y. Yin, Q. Li, Atomic layer deposition of Al₂O₃ and Al₂O₃/TiO₂ barrier coatings to reduce the water vapor permeability of polyetheretherketone, *Thin Solid Films* 591 (Part A) (2015) 131–136.
17. P.S. Maydannik, T.O. Kääriäinen, K. Lahtinen, D.C. Cameron, M. Söderlund, P. Soininen, P. Johansson, J. Kuusipalo, L. Moro, X. Zeng, Roll-to-roll atomic layer deposition process for flexible electronics encapsulation applications, *J. Vac. Sci. Technol. A* 32 (2014) 051603.
18. Yoshida, H.; Ebina, T.; Arai, K.; Kobata, T.; Ishii, R.; Aizawa, T.; Suzuki, A. Development of Water Vapor Transmission Rate Measuring Device Using a Quadrupole Mass Spectrometer and Standard Gas Barrier Films down to the 10⁻⁶ g m⁻² day⁻¹ Level. *Review of Scientific Instruments* **2017**, 88 (4), 043301.
19. Hülsmann, P.; Philipp, D.; Köhl, M. Measuring Temperature-Dependent Water Vapor and Gas Permeation through High Barrier Films. *Review of Scientific Instruments* **2009**, 80 (11), 113901.
20. Brewer, P. J., Goody, B. A., Kumar, Y. & Milton, M. J. Accurate measurements of water vapor transmission through high-performance barrier layers. *Rev. Sci. Instrum.* 83, 075118 (2012).
21. Nisato, G.; Klumbies, H.; Fahlteich, J.; Müller-Meskamp, L.; van de Weijer, P.; Bouten, P.; Boeffel, C.; Leunberger, D.; Graehlert, W.; Edge, S.; Cros, S.; Brewer, P.; Kucukpinar, E.; de Girolamo, J.; Srinivasan, P. Experimental Comparison of High-

- Performance Water Vapor Permeation Measurement Methods. *Organic Electronics* **2014**, *15* (12), 3746–3755.
22. Higgs, D. J.; Young, M. J.; Bertrand, J. A.; George, S. M. Oxidation Kinetics of Calcium Films by Water Vapor and Their Effect on Water Vapor Transmission Rate Measurements. *The Journal of Physical Chemistry C* 2014, *118* (50), 29322–29332.
23. Klumbies, H.; Müller-Meskamp, L.; Mönch, T.; Schubert, S.; Leo, K. The Influence of Laterally Inhomogeneous Corrosion on Electrical and Optical Calcium Moisture Barrier Characterization. *Review of Scientific Instruments* **2013**, *84* (2), 024103.
24. Bora, M. Non-Destructive, in-Situ Evaluation of Water Presence Using Thermal Contrast and Cooled Detector. 11448555, September 20, 2022.
25. Bora, M.; Kotovsky, J. Non-Destructive Evaluation of Water Ingress in Photovoltaic Modules. 9588058, March 7, 2017.
26. Lian, S.; Zhang, J.; Wang, J.; Xu, C.; Swart, H. C.; Terblans, J. J. A Model for Adsorption and Diffusion in Water Vapor Barrier Films. *physica status solidi (b)* **2021**, *258* (6), 2000609.
27. G. L. Graff, P. E. Burrows, R. E. Williford, R. F. Praino, in *Flexible Flat Panel Displays* (Ed. G.P. Crawford), John Wiley & Sons, Chichester 2005.
28. Jarvis, K. L.; Evans, P. J.; Cooling, N. A.; Vaughan, B.; Habsuda, J.; Belcher, W. J.; Bilen, C.; Griffiths, G.; Dastoor, P. C.; Triani, G. Comparing Three Techniques to Determine the Water Vapour Transmission Rates of Polymers and Barrier Films. *Surfaces and Interfaces* **2017**, *9*, 182–188.

29. Dameron, A. A.; Davidson, S. D.; Burton, B. B.; Carcia, P. F.; McLean, R. S.; George, S. M. Gas Diffusion Barriers on Polymers Using Multilayers Fabricated by Al₂O₃ and Rapid SiO₂ Atomic Layer Deposition. *The Journal of Physical Chemistry C* **2008**, *112* (12), 4573–4580.



(a)



(b)

Figure 1. (a) Image of instrument setup. (b) Schematic of instrument step. Moisture barrier samples were fabricated by deposition of barrier film on the polymer substrate. For testing, the polymer substrate side was sealed with 1 μm thick impermeable layer of copper followed by glass slide mounted with epoxy. The sample was illuminated with a black body and imaged in transfection mode with a custom-made infrared camera. The light passed twice through the polymer substrate and was attenuated in proportion to the water content present in the polymer.

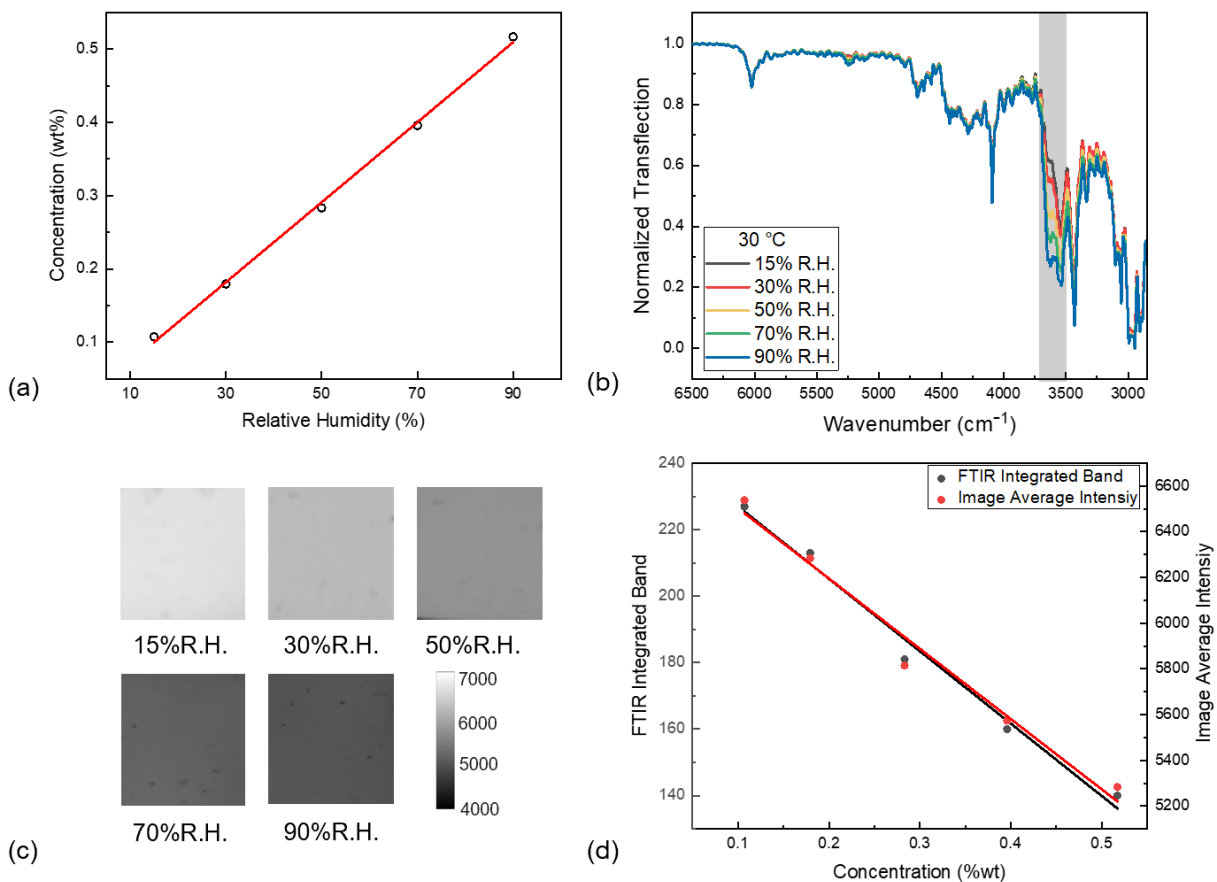


Figure 2. Calibration of water content in the PET substrate showing a) the Karl-Fisher titration measured water concentration in PET substrate equilibrated in moist air at selected RH values and 30°C, and b) the normalized FTIR transflection spectra from IR passage through the substrate for the same equilibrated conditions as above. The highlighted wavelengths correspond to the water absorption band. c) Sample images indicate decreased image intensity due to water absorption at the 3700 to 3500 cm^{-1} . d) The linear dependence of the integrated FTIR water absorption band and the average image intensity as a function of the absolute Karl-Fisher water concentration (black corresponds to FTIR integration, red to image average intensity).

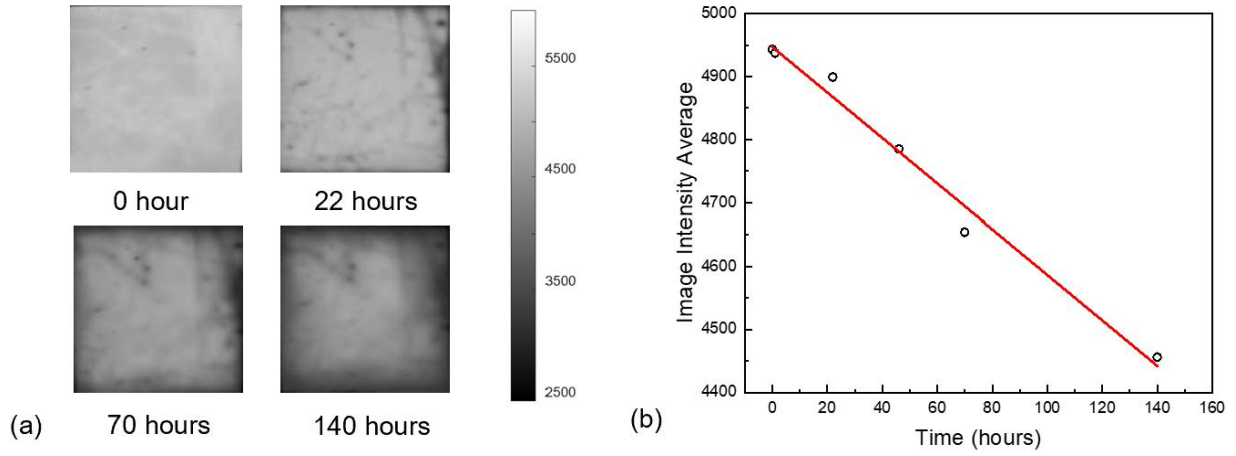


Figure 3. Visualization of defects present in the moisture barrier after exposure to 38°C and 90% relative humidity showing (a) Infrared images at different exposure time, and (b) decrease image intensity average due to moisture ingress across the barrier and from the exposed perimeter as a function of time.

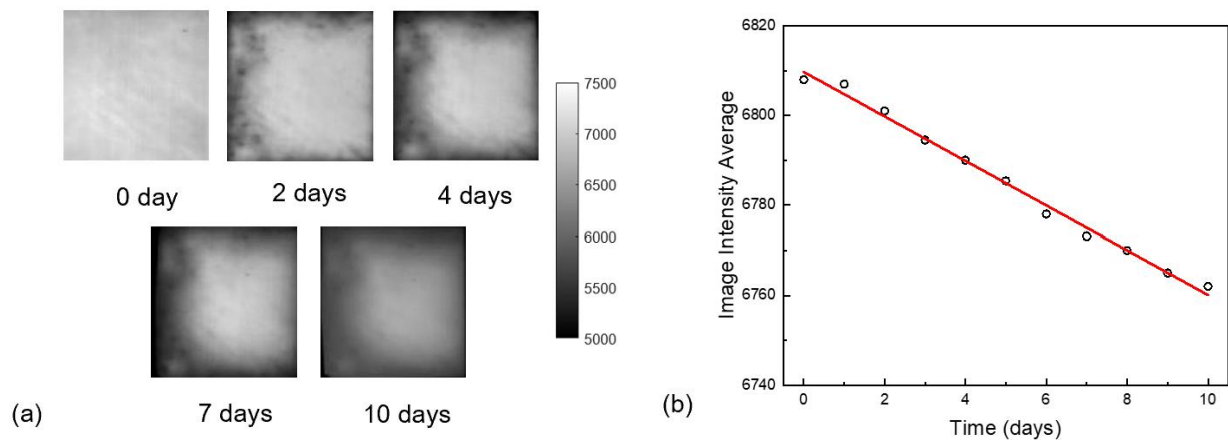


Figure 4. WVTR values were calculated for moisture barriers after aging under 38 °C and 90 % R.H. (a) Infrared images of the samples were acquired every day after exposure to the aging condition. (b) The corresponding image intensity average change over time was determined from image processing excluding the edges of the sample, indicating decrease in intensity with longer aging time. WVTR value of the barrier calculated from IR imaging method is $9.6 \cdot 10^{-4} \text{ g/m}^2/\text{day}$.

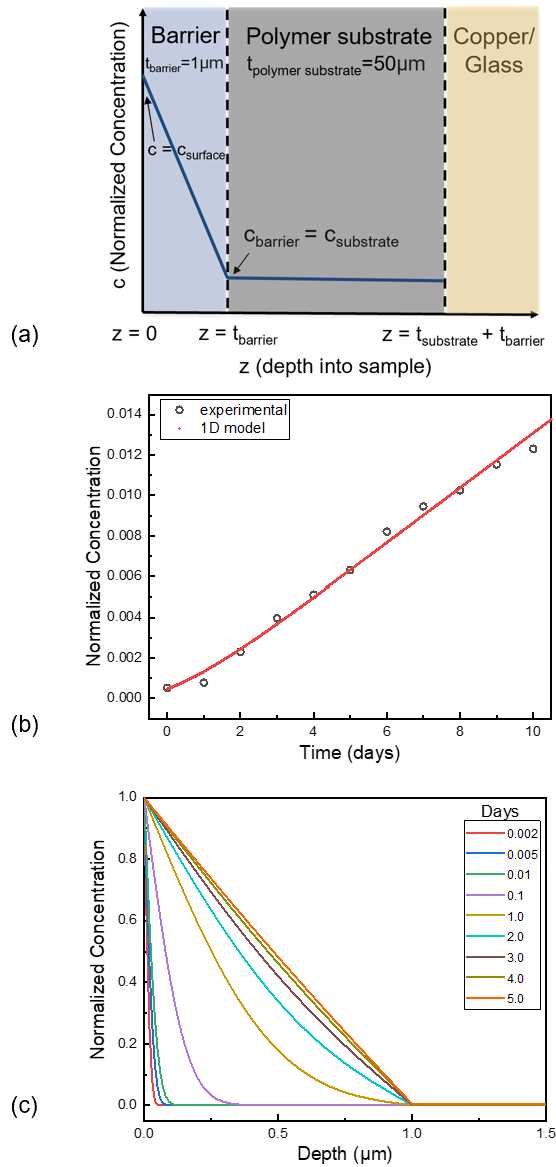


Figure 5. Numerical simulation of water transport in the moisture barrier and fitting with experimental data. a) The sample is modelled with two domains: the PET polymer substrate and a barrier layer with lower diffusion coefficient. The air side of the barrier is kept at saturation while at the interface between the two domains the relative concentration is continuous, and it's assumed that there is no water flux on the polymer substrate side that is sealed with a uniform copper layer. b) Numerical fit for the moisture diffusion data was derived from the infrared imaging measurement results. The fit uses the model presented in a) and calculates the diffusion coefficient in the barrier using a least square algorithm. c) Diffusion profiles for water concentration in the sample at various times. The water diffusion front passes through the barrier layer until it reaches a linear profile. The water concentration in the substrate is uniform as the diffusion coefficient in this material is orders of magnitude higher than the one in the barrier.

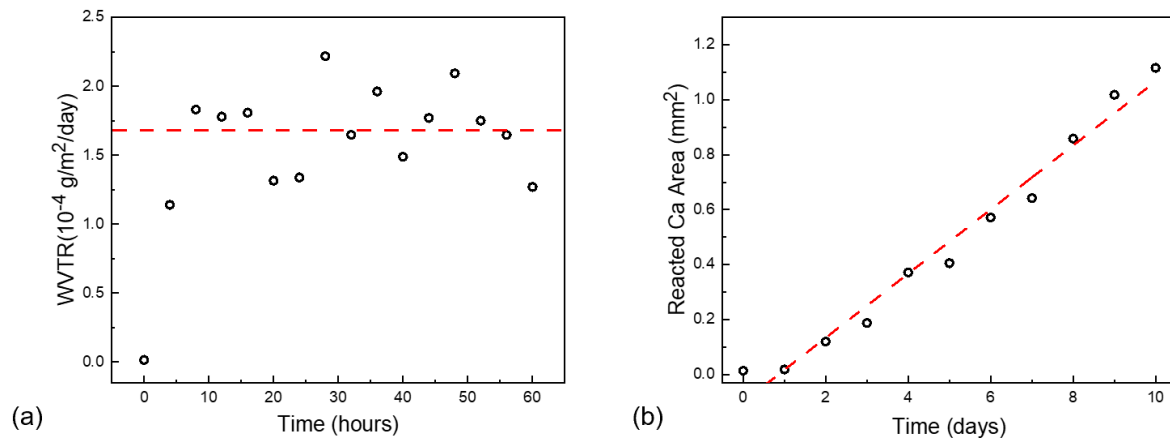


Figure 6. WVTR measurement of moisture barriers with permeation method and optical calcium film method. (a) WVTR values measured from permeation method show average at $1.7 \cdot 10^{-4} \text{ g/m}^2/\text{day}$ (dashed line), with a coefficient of variation of 18%. (b) WVTR values determined from optical calcium testing showing the total reacted calcium area over time under the same exposure condition as above. The WVTR of the barrier was derived from calculating the equivalent amount of water needed to react the calcium layer showing the value around $8.5 \cdot 10^{-4} \text{ g/m}^2/\text{day}$.

Measurement method	WVTR(g/m ² /day)
Infrared imaging	$9.6 \cdot 10^{-4}$
Permeation	$1.7 \cdot 10^{-4}$
Optical calcium film	$8.5 \cdot 10^{-4}$

Table 1. A comparison of the WVTR results measured from Infrared imaging, permeation method and optical calcium film method.